FUNDAMENTALS OF THE GLA PHYSICAL RETRIEVAL METHOD

Moustafa T. Chahine
Jet Propulsion Laboratory
California Institute of Technology
Pasadena, CA USA

Joel Susskind
Goddard Space Flight Center
Greenbelt, MD USA

1. ABSTRACT

HIRS2/MSU data are analyzed at GLA using a physically based technique which directly accounts for all factors affecting the radiances other than cloud effects. All radiative transfer calculations are performed at the satellite zenith angle of observation. Cloud effects are handled indirectly using observations in adjacent fields of view which are assumed to be otherwise homogeneous, except for degree of cloudiness. The treatment of clouds in the GLA physical retrieval algorithm is carried out analytically without requiring any field of view to be necessarily clear. The algorithm permits determination of atmospheric temperature profiles accurately under most cloud conditions, and shows little degradation in the number of accepted retrievals and their accuracy as a function of increased cloudiness or satellite zenith angles. "Microwave only" retrievals are never performed.

2. INTRODUCTION

The Goddard Laboratory for Atmospheres (GLA) physical retrieval algorithm is based on the relaxation method of solution of the full radiative transfer equation by Chahine (1968, 1970, 1974 and 1982). Several improvements and modifications have been added by Susskind, et al. (1984, 1985, 1987), and Reuter et al. (1988) resulting in the final algorithm used in this study. Briefly, the GLA physical retrieval algorithm begins with a first guess field of atmospheric temperature and humidity and modifies these profiles according to the difference between the observed radiances, which are corrected for cloud effects, and those computed from the first guess. The process is repeated until the residuals between the measured and calculated radiances approach a small asymptotic value. In general, a good first guess reduces the

number of iterations required and minimizes the impact of noise and other uncertainties on the final solution. The first guess in the current retrieval package is obtained from the six-hour forecast field generated by the General Circulation Model (GCM) of the Goddard Laboratory for Atmospheres. The model is run interactively with the retrieval as described in Susskind and Pfaendtner (1989) elsewhere in this volume. Details of this GCM are given by Kalnay, et al. (1983).

For each six-hour period, the interactive cycle of the iterative relaxation solution starts with the six-hour forecast fields of atmospheric temperature and humidity generated by the GCM. The forecast fields are then applied as a first guess for all soundings occurring within ±3 hours of the forecast time. In the algorithm, we express the retrieved temperature profiles as perturbation solutions around a mean temperature profile as discussed by Susskind, et al. (1984). We have observed that the resulting solutions do not depend appreciably on the initial guess in those layers where the weighting functions peak. Thus, the GCM initial guess tends to help the solution in those layers where the HIRS2/MSU information is weak. The set of sounding frequencies shown in Table 1 corresponds to the channels of the HIRS2 and MSU sounders on the NOAA operational low Earth orbiting satellites. They monitor emission arising primarily from the Earth's surface and the atmosphere up to the mid-stratosphere. The pressure from which most of the radiance arises, as well as its principle use, is also shown for each channel in table 1. The main absorber in window channels is also indicated. These infrared and microwave channels provide the basic remote sensing information used in the retrieval algorithm.

3. OVERVIEW

An extremely important step in deriving the atmospheric temperature profile T(p) is the determination of the clear-column radiances (or brightness temperatures), which are the radiances emerging from the clear portions of the scene. The infrared channels are used, together with microwave channels sounding the troposphere and stratosphere, to determine the clear-column temperature profiles from the clear column radiances, while the lower atmospheric sounding microwave channel is used to account for the effects of clouds on the IR observations. These two steps are carried out simultaneously. The objective is to determine the clear-column temperature profiles such that the resulting T(p) yields calculated brightness temperature values which agree well both with the measured microwave values, which are not cloud contaminated, and the cloud corrected IR values. The resulting temperature profiles derived by this approach do not show appreciable degradation due to clouds, even for up to 85% cloudiness, as shown in simulation studies by Phillips et al., (1988) and with real data in this paper.

Table 1. HIRS2 and MSU Channels

Channel	Frequency cm^{-1}	Peak of $d\tau / d\ln p$ mb	Function
H1	668.40	30	not used
H2	679.20	60	T(p)
H3	691.10	100	not used
H4	703.60	280	T(p), clouds
H5	716.10	475	clouds
H6	732.40	725	clouds
H7	748.30	Surface	clouds
H8	897.70	Window *(water)*	Surface temp. and q(p)
H9	1027.90	Window *(ozone)*	Ozone burden
H10	1217.10	(v) 1000	q(p)
H11	1363.70	(v) 600	q(p)
H12	1484.40	(v) 400	q(p)
H13	2190.40	Surface	T(p), cloud correction
H14	2212.60	650	T(p), cloud correction
H15	2240.10	340	T(p)
H16	2276.30	170	not used
H17	2310.70	15	not used
H18	2512.00	Window *(nitrogen)*	surface temp.
H19	2671.80	Window *(water)*	surface temp.
M1	50.30GHz	Window	Surface emissivity
M2	53.74	500	Cloud correction
M3	54.96	300	T(p)
M4	57.95	70	T(p)

(v) variable

The basic steps of the GLA physical relaxation algorithm are:

(1) Calibration of the data.

(2) Grouping of data, within a given horizontal grid size of 2x2 HIRS2 footprints, according to degree of cloudiness in the field-of-view of each footprint.

(3) Attaching initial guess (superscript $n=0$) of temperature profile, $T^0(p)$, humidity profile $q^0(p)$, surface skin temperature T_s^0, and surface pressure p_s.

(4) Computation of clear-column radiances $I^{o}(\upsilon_i)$, for each sounding frequency (υ_i) from the initial guess conditions, [see Eq. (1)].

(5) Determination of the surface emissivity at 50.3 GHz to compute microwave radiances for the cloud filtering atmospheric channels, [see Eq. (32) in Susskind et al. (1984)].

(6) Reconstruction of the clear-column infrared radiance $\bar{I}^{n}(\upsilon_i)$ from potentially cloud-contaminated radiance measurements, [see Section 5.1].

(7) Determination of T_s^n, the iterative sea/land surface temperature, [see section 6.1].

(8) Determination of the new (n+1) iterative temperature profile, [use Eq. (24)].

(9) Calculation of $I^{n+1}(\upsilon_i)$, the clear-column radiances computed using the iterative sea/land surface temperature and temperature profile, [use Eq. (1)].

(10) Comparison of $\bar{I}^{n+1}(\upsilon_i)$ and $I^{n+1}(\upsilon_i)$ to obtain the residuals for the temperature sounding channels. [see section 5.4].

(11) If sufficient agreement is not found in step 10, calculate the next iterative temperature profile and return to step 5 to compute the microwave surface emissivity; and continue the iterative procedure. Otherwise, the iterative procedure is terminated.

(12) Application of criteria to accept or reject retrieved profiles, [see Section 6.2].

(13) Calculation of humidity and ozone profiles

(14) Calculation of cloud fields and other parameters.

Our main concern in this paper is in the factors most directly related to the computation of atmospheric temperature profiles. Steps 13 and 14 are done subsequent to the determination of $T(p)$ and will not be discussed.

3.1 Important notations

Treatment of the effects of clouds on radiances, as well as the computation of radiances expected as a function of geophysical conditions, are very important aspects of the method. The following four forms of the radiance I corresponding to a given frequency υ, order of iteration n, and field-of-view k, are used in this paper. Each form will be defined separately in the text, however, it is helpful to define them together here:

$\tilde{I}_k(\upsilon)$ is the **measured** radiance corresponding to fields-of-view k (not necessarily assumed to be cloud-free).

$I^n(\upsilon)$ is the clear-column radiance **computed** from the radiative transfer equation using the nth iterative temperature profile $T^n(p)$ [see Eq. (1)].

$\bar{I}^n(\upsilon)$ is the clear-column radiance **reconstructed** from observations over adjacent fields-of-view according to Eq. (6). It represents the radiance emerging from the clear portions of the fields-of-view.

$\bar{I}^n_a(\upsilon')$ is the **adjusted** clear column radiance of the infrared cloud-filtering channel υ'. It is used only to determine the cloud correction coefficient η^n, used to determine clear-column radiances for all channels. [see Section 5.1].

In the text, $I^n(\upsilon)$ represents what the nth estimate of the clear-column radiance is, while $\bar{I}^n(\upsilon)$ represents what the clear column radiance should be at the same iteration. The iterative solution converges when $I^n(\upsilon) \rightarrow \bar{I}^n(\upsilon)$.

Identical notations are used for the brightness temperature, namely: $\tilde{\Theta}_k(\upsilon)$, $\Theta^n(\upsilon)$, $\bar{\Theta}^n(\upsilon)$, *and* $\bar{\Theta}^n_a(\upsilon')$.

4. TREATMENT OF RADIANCES IN CLOUDY ATMOSPHERES

The measured radiance is a function of the thermal state of the atmosphere, the concentration of radiatively active gases, properties of the earth's surface, the extent, heights and radiative transfer properties of clouds and aerosols, and the satellite zenith angle of observation. By treating the cloud effects as short-period oscillations over the clear-column radiance, an analytical method was developed by Chahine (1974, 1977, 1982) to retrieve clear-column vertical temperature

profiles from radiance measurements made in the presence of clouds. The method requires radiance data from two spectral regions measured over two adjacent fields-of-view, otherwise identical but having different amounts of clouds, to infer the radiances being emitted from the clear portions of the scene. The uncoupling of the effects of clouds is carried out analytically without a-priori information about the amounts, heights and types of clouds in the fields-of-view.

4.1 Computed clear column radiance

For a general treatment of the problem, we consider the radiance, $\hat{I}(\upsilon)$, at frequency υ measured in the presence of clouds. In addition, we can express the clear-column radiance expected as a function of geophysical parameters, $I(\upsilon)$, in terms of its four components. They are the surface emission, the atmospheric emission, the reflected downward-flux, and the reflected solar radiation, shown respectively in the four terms on the right-hand side of Eq. (1).

$$
\begin{aligned}
I(\upsilon) = {} & \varepsilon_s(\upsilon)\, B(\upsilon, T_s)\, \tau(\upsilon, p_s) \\
& + \int_{p_s}^{0} B[\upsilon, T(p)] \, \frac{\partial \tau(\upsilon, p)}{\partial \ln p} \, d\ln p \\
& + \Omega(\upsilon) \cos\theta \, [1 - \varepsilon_s(\upsilon)] \, I_d(\upsilon, 0)\, \tau(\upsilon, p_s) \\
& + H_h(\upsilon) \cos\phi_h \, \tau'(\upsilon, \phi_h, \theta)\, \rho_s(\upsilon_j, \phi_h, \theta)
\end{aligned}
\qquad (1)
$$

Eq. (1) can be used to compute the clear-column radiance for any satellite zenith angle θ. In Eq. (1), $\tau(\upsilon,p)$ is the channel-averaged transmittance of a clear-column of gaseous absorbers between pressure level p and the sounder; $\varepsilon_s(\upsilon)$ is the surface emissivity, p_s is the surface pressure, T_s is the surface skin temperature, B the Planck black-body function, and $T(p)$ the clear-column vertical temperature profile. The term $I_d(\upsilon,0)$, representing downwelling thermal radiation, is taken as

$$
I_d(\upsilon, 0) = \int_{p_s}^{0} B[\upsilon, T(p)] \, \frac{\partial \tau(\upsilon, p)}{\partial \ln p} \, d\ln p
$$

computed at the nadir angle, and $\Omega(\upsilon)$ is a geometrical form factor which is equal to 2 in the window regions where the atmosphere is optically thin. $\Omega(\upsilon)$ is parameterized for other channels as in Susskind et al. (1983). In the last term, $\tau(\upsilon, \phi_h, \theta)$ is the transmittance along the

path of the solar incident radiation to the surface and back to the satellite, ϕ_h is the sun angle, $H_h(\upsilon)$ is the solar black body radiation corresponding to a temperature of 5600 K, and $\rho_s(\upsilon_j,\phi_h,\theta)$ is the bidirectional surface reflectance (including the effects of solar obscuration by clouds). Further details of how all terms are treated, as well as the accuracy of the calculation, are shown in Susskind et al. (1983).

4.2 Reconstructed clear column radiance

If we consider observations made over two adjacent fields-of-view $\tilde{I}_1(\upsilon)$ and $\tilde{I}_2(\upsilon)$ which are thought to be homogeneous except for cloud cover, and if

$$\tilde{I}_1(\upsilon) \neq \tilde{I}_2(\upsilon)$$

we attribute this difference to differences in cloudiness in the two fields-of-view. We will also assume their corresponding (reconstructed) clear-column radiances to be relatively the same, i.e.,

$$\hat{I}_1(\upsilon) \approx \hat{I}_2(\upsilon) = \hat{I}(\upsilon)$$

The term "reconstructed clear-column radiance" $\hat{I}(\upsilon)$ may be viewed as representing the radiance emitted from the clear-portions of any field-of-view, normalized to unit area. In other words, it is what the measured radiance would have been if it were not for the interference of the clouds. Thus, the cloud effect can now be expressed as the difference between the reconstructed clear-column radiance and the measured radiance, $[\hat{I}(\upsilon)-\tilde{I}(\upsilon)]$, for any given field-of-view.

Several mathematical filtering techniques can be employed to eliminate the effects of clouds. One physically intuitive approach suggests an expansion of the ratio of the cloud effects in adjacent fields-of-view as

$$\frac{\hat{I}(\upsilon)-\tilde{I}_1(\upsilon)}{\hat{I}(\upsilon)-\tilde{I}_2(\upsilon)} = c_o + c_1 F(\upsilon,d,...) + ..., \qquad (2a)$$

where F is some expansion function (yet undefined), c_o and c_1 are expansion coefficients independent of frequency, and d is a parameter.

According to Eq. (2a), c_0 is a scaling coefficient representing the degree of linear similarities (i.e., homogeneity) between the clouds in the adjacent fields-of-view. All other effects, due to cloud inhomogeneities, are accounted for by expansion function terms of which only one is shown here. The physical meaning of c_1 and d cannot be defined now because the form of F is left undetermined.

The next step is to eliminate the high-frequency components represented by $F(\upsilon,d,...)$. This step is accomplished by considering a third field-of-view and writing

$$\frac{\bar{I}(\upsilon)-\tilde{I}_2(\upsilon)}{\bar{I}(\upsilon)-\tilde{I}_3(\upsilon)} = c'_o + c'_1 F(\upsilon,d,...) + ..., \qquad (2b)$$

then proceeding to eliminate the expansion function $F(\upsilon,d,...)$ between Eqs. (2a) and (2b). The resulting linear equation relates the reconstructed clear-column radiance, $\hat{I}(\upsilon)$, to the measured radiances, $\tilde{I}_1(\upsilon)$,$\tilde{I}_2(\upsilon)$, and $\tilde{I}_3(\upsilon)$, as

$$\hat{I}(\upsilon) = \tilde{I}_1(\upsilon) + \eta_1[\tilde{I}_1(\upsilon) - \tilde{I}_2(\upsilon)]$$

$$+ \eta_2[\tilde{I}_1(\upsilon) - \tilde{I}_3(\upsilon)] + ..., \qquad (3)$$

where η_1 and η_2 are two unknown constants independent of frequency.

Note that so far we have not made any assumptions about F and we have not required any field-of-view to be cloud free. The only condition required to derive Eq. (3) is

$$\tilde{I}_1(\upsilon) \neq \tilde{I}_2(\upsilon) \neq \tilde{I}_3(\upsilon) \qquad (4)$$

The observational requirements needed to satisfy Eqs. (3) and (4) are that all sounding frequencies should see the same field-of-view at the same time and that the fields-of-view should be close together so as to represent areas which are similar except for cloud amount.

Another mathematical filtering approach may be derived by expanding the cloud effects directly in terms of some expansion function, $G(\upsilon,p,...)$, as

$$\bar{I}(\upsilon) - \tilde{I}_1(\upsilon) = N_1 G(\upsilon,p,...) + N'_1 G'(\upsilon,p,...) + ..., \qquad (5)$$

$$\hat{I}(\upsilon) - \tilde{I}_2(\upsilon) = N_2 G(\upsilon,p,...) + N'_2 G'(\upsilon,p,...) + ...$$

where $G(\upsilon,p,...)$ and $G'(\upsilon,p,...)$ are two terms of some expansion function, N_1, N'_1, N_2, and N'_2 are the expansion coefficients, and the subscript refers to the field-of-view. Eq. (5) is conceptually equivalent to Eqs. (2a) and (2b) and can be reduced to yield Eq. (3), subject to the same condition given in Eq. (4).

In general, for the HIRS2/MSU data, we have observed that the cloud coefficient η_2 is one or two orders of magnitude smaller than η_1. Thus, one expansion term of Eq. (5) seems to be sufficient to define the clear-column radiance for the purposes of the HIRS2/MSU system. The resulting expression for the clear-column radiance, after dropping the subscript for η, becomes

$$\hat{I}(\upsilon)=\tilde{I}_1(\upsilon)+\eta[\tilde{I}_1(\upsilon)-\tilde{I}_2(\upsilon)] \tag{6}$$

η is related to N_1 and N_2 as $\eta = N_1/(N_1 - N_2)$. When the exact value η is substituted in Eq. (6), $\hat{I}(\upsilon)$ becomes equal to the term which should be used in the left hand side of Eq. (1).

$$I(\upsilon)=\hat{I}(\upsilon) \tag{7}$$

The numerical value for η can be determined [see Chahine (1974), section 3] by selecting a cloud dependent tropospheric channel, say υ', from the long-wave part of the spectrum, and substituting into Eq. (6) to get

$$\eta=\frac{\bar{I}(\upsilon')-\bar{I}_1(\upsilon')}{\bar{I}_1(\upsilon')-\bar{I}_2(\upsilon')} \tag{8}$$

Since η is independent of frequency, it can be used to reconstruct the clear-column radiance, $\hat{I}(\upsilon)$, for all sounding frequencies which observed the same field-of-view. In order to get an accurate value of η, we first need an accurate estimate of $\hat{I}(\upsilon')$, the expected clear column radiances.

5. BASIC RETRIEVAL APPROACH

It is useful to write the full expression for Eq. (6) as

$$\begin{aligned}\hat{I}(\upsilon_j)&=\tilde{I}_1(\upsilon_j)+\eta[\tilde{I}_1(\upsilon_j)-\tilde{I}_2(\upsilon_j)]\\ &=\varepsilon_s(\upsilon_j)\ B(\upsilon_j,T_s)\ \tau(\upsilon_j,p_s)\\ &+\int_{p_s}^{0} B[\upsilon_j,T(p)]\ \frac{\partial\tau(\upsilon_j,p)}{\partial\ln p}\ d\ln p\\ &+\Omega\cos\theta\,[1-\varepsilon_s(\upsilon_j)]I_d(\upsilon_j,0)\,\tau(\upsilon_j,p_s)\\ &+H_h(\upsilon_j)\cos\phi_h\ \tau'(\upsilon_j,\phi_h,\theta)\ \rho_s(\upsilon_j,\phi_h,\theta)\end{aligned} \tag{9}$$

The retrieval problem is now concisely stated in Eq. (9): From a given set of radiance measurements $\tilde{I}_1(\upsilon_j)$ and $\tilde{I}_2(\upsilon_j)$, determine the unknowns η, $\varepsilon_s(\upsilon_j)$, $\rho_s(\upsilon_j,\phi_h,\theta)$, T_s, and $T(p)$.

The determination of the clear column radiance, $\hat{I}(\upsilon)$ (or η) is carried out simultaneously with the determination of the clear column temperature and humidity profile. The basic aspects of the solution will be described in the rest of this section.

5.1 Determination of η from microwave data

When radiances from a single spectral region are used, Eq. (9) possesses an infinite number of solutions; one for each given value of η as illustrated in Fig. 1. We aim then to chose the value of η which produces a temperature profile satisfying a given microwave atmospheric channel. Microwave sounding frequencies, which are sensitive to tropospheric temperature profiles and are not affected by hazes and most types of clouds, are preferable over long-wave IR frequencies for determination of the clear-column radiance. In this step η is determined by iteration until the resulting clear-column temperature profile yields calculated microwave brightness temperature values which agree well with the measured values for the selected microwave atmospheric channel.

To accomplish this, we couple the convergence of a selected atmospheric microwave channel υ'' (channel 2 of MSU) to that of a selected infrared channel υ' (channel 13 from the HIRS). We write this simple relationship in the brightness temperature domain as

$$\overline{\Theta}_a^n(\upsilon') = \Theta^n(\upsilon') + [\tilde{\Theta}(\upsilon'') - \Theta^n(\upsilon'')] \qquad (10)$$

Eq. (10) states that at the nth iteration, the brightness temperature for the infrared cloud filtering channel, υ', is **adjusted** from its calculated value at the same iteration by an amount equal to the difference between the measured and calculated brightness temperatures of the selected microwave channel υ''. Eq. (10) relaxes the temperature profile in the n+1 iteration towards better agreement with the measured microwave data.

The brightness temperature, Θ, is related to the radiance, $I(\upsilon)$, as

$$I(\upsilon) = \alpha\, \upsilon^3 / [\exp(\beta\, \upsilon / \Theta) - 1] \qquad (11)$$

where α and β are constants. Thus, we can immediately calculate the corresponding corrected radiance in υ' by substituting Eq. (10) into Eq. (11) to yield

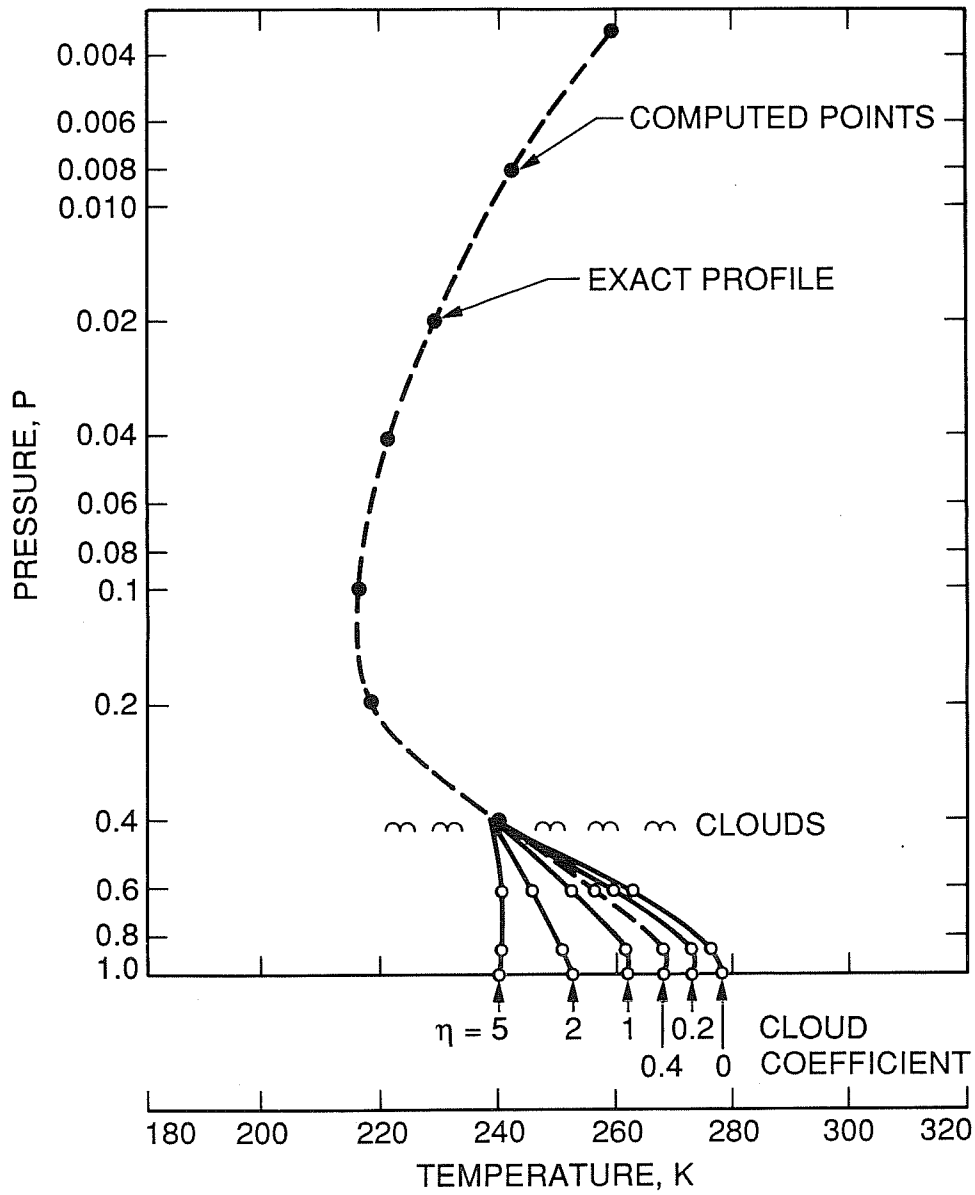

Figure 1 Clear column temperature profiles consistent with different sets of clear column radiances obtained from measurements in two fields of view assuming different values of η. The cloud level is indicated. Errors in η can produce large temperature errors beneath the cloud.

$$\bar{I}_a^n(\upsilon') = \alpha \upsilon'^3 / \{\exp[\beta \upsilon' / \bar{\Theta}_a^n(\upsilon')] - 1\} \qquad (12)$$

The nth iterative value of the cloud coefficient η^n is obtained by substituting the resulting corrected value of the radiance in channel υ' into Eq. (8) to get

$$\eta^n = \frac{\bar{I}_a^n(\upsilon') - \bar{I}_1(\upsilon')}{\bar{I}_1(\upsilon') - \bar{I}_2(\upsilon')} \qquad (13)$$

The resulting cloud coefficient η^n can be used to reconstruct the clear-column radiance according to Eq. (6) for any sounding frequency which observed the same field-of-view simultaneously with channel υ'. Large values of η, when used in Eq. (9), amplify observation noise and can produce potentially large errors in reconstructed clear column radiances. Therefore, if $\eta > 4$ the scene is either flagged as too cloudy to perform a retrieval, or is called clear (η is set equal to -0.5, for which value $\tilde{I} = [\tilde{I}_1 + \tilde{I}_2]/2$) if certain conditions are met (Susskind et al., 1984).

5.2 The relaxation transformation

To solve Eq. (9) for the determination of $T(p)$, we will first map each sounding frequency υ_j into a specific pressure level p_j where p_j corresponds to the peak value of the kernel $d\tau(\upsilon,p)/d\ln p$. Mathematically, we have now derived the transformation of the $\upsilon-axis$ into the p-axis as

$$\upsilon_j = \upsilon(p_j) \qquad (14)$$

Next, we will map the I-axis into the T-axis. This is much more difficult, however, and needs to be carried out by iteration. We apply the mean value theorem [Chahine, 1968, 1970] and derive a relaxation equation of the form

$$\frac{T^{n+1}(p_j)}{T^n(p_j)} = \frac{\bar{I}(\upsilon_j)}{I^n(\upsilon_j)} \qquad (15)$$

5.3 Numerical constraints

Equation (15) gives estimates of temperature profile at discrete points. Selecting numerical constraints for interpolation is not trivial, particularly in cases where the number of measured radiances is small. Application of the relaxation method of solution to a variety of problems has shown that the resulting solutions are not highly dependent of the initial guess but depend on the interpolation formula selected. The selection of a suitable constraint is basically subjective.

The approach used at GLA selects constraints in the form of Empirical Orthogonal Functions (EOFs). Other methods, which preserve the shape of the initial guess, are also very useful. The EOF interpolation procedure will be discussed in detail in section 6.

5.4 Properties of the residuals

We define the "residuals" of the solution as the rms difference between $\bar{I}^n(\upsilon_j)$ and $I^n(\upsilon_j)$ for all the temperature sounding frequencies as

$$R^n_{rms} = \left[\frac{\bar{I}^n(\upsilon_j) - I^n(\upsilon_j)}{\bar{I}^n(\upsilon_j)}\right]_{rms} \qquad (16)$$

The equivalent form of the residuals in the brightness temperature domain is given in Eq. (29).

Examination of the residuals shown in Fig. 2 reveals that the residuals tend toward different asymptotic values according to the values of the corresponding noise in observations. For zero noise, the asymptotic value is equal to the quadrature errors. However, in the presence of errors in measurements, the residuals first decrease and then approach an asymptotic value of the same order of magnitude as the errors in measurements. This property suggests that the iterative process should be terminated when the residuals begin to approach their asymptotic value.

6. APPLICATION TO HIRS2/MSU CHANNELS

The steps used in the GLA physical retrieval algorithm to solve the radiative transfer equation are described by Susskind, et al. (1984). In this algorithm the relaxation approach is derived in the brightness temperature domain rather than the radiance domain. This modification was used because it provides a simpler physical interpretation, and because brightness temperature is more linearly related to differences in temperature profiles.

In order to obtain the form of the relaxation equation which will be used in the algorithm, we first relate the brightness temperature, $\Theta(\upsilon)$, to the radiance, $I(\upsilon)$, as in Eq. (11)

$$\Theta(\upsilon) = \beta\upsilon / \{\ln[\alpha\upsilon^3/I(\upsilon)] - 1\} \qquad (17)$$

Where α and β are constants. The corresponding form of the relaxation equation Eq. (15) is

$$T^{n+1}(p_j) = T^n(p_j) + [\overline{\Theta}^n(\upsilon_j) - \Theta^n(\upsilon_j)] \qquad (18)$$

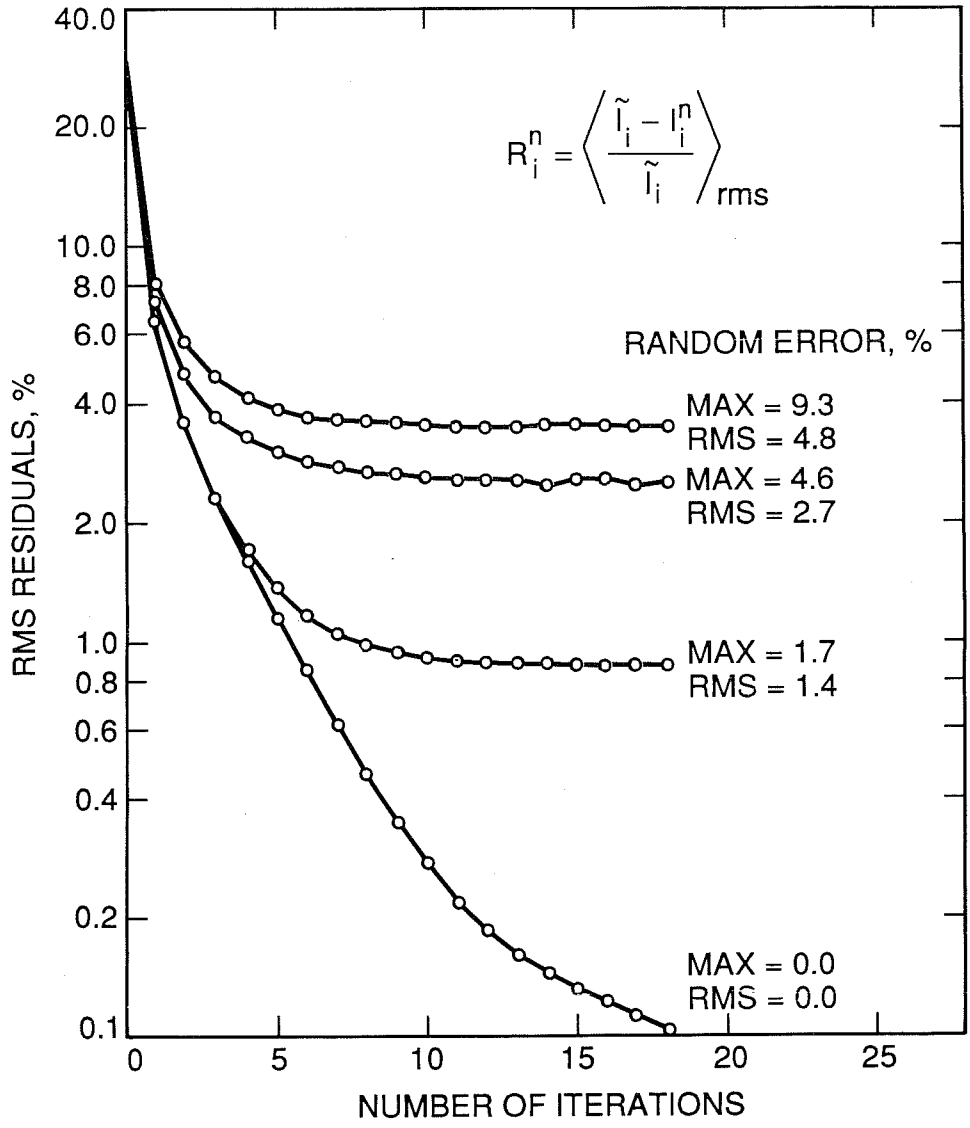

Figure 2 Residuals of the relaxation solution to a simulated set of radiances as a function of simulated noise levels and iteration. Characteristics of the radiance noise is shown for each curve.

where:

$T^{n+1}(p_j)$ is the temperature at pressure level p_j corresponding to the n+1 iteration

$T^n(p_j)$ is the nth iterative temperature at pressure level p_j

$\overline{\Theta}^n(\upsilon_j)$ is the nth iterative reconstructed brightness temperature corresponding to frequency υ_j.

$\Theta^n(\upsilon_j)$ is the nth calculated brightness temperature for frequency υ_j corresponding to the nth iterative temperature profile $T^n(p)$

In the GLA algorithm, rather than rely on just one frequency to give an estimate of the updated temperature profile at pressure $T^{n+1}(p_j)$, we apply weighting coefficients, $W_i(p_j)$, using information from other frequencies. The expression for the weighting coefficients, $W_i(p_j)$, is given by Susskind, et al. (1984), as

$$W_i(p_j) = [\frac{dB_i}{dT}]^{-1}_{T=\Theta_i} \quad [\frac{dB_i}{dT}]_{T(p)} \quad [\frac{d\tau_i}{d\ln p}]_p \qquad (19)$$

$W_i(p_j)$ represents the sensitivity of brightness temperature in channel i to changes in temperature at pressure p_j. It depends on all geophysical parameters as well as the zenith angle of observation.

The use of weighting coefficients reduces the effects of noise and improves the stability of the solution. In addition, the iterative equation is performed on layer mean temperatures. The resulting form of the relaxation equation applied to retrieve layer mean temperature values becomes

$$\hat{T}^{n+1}(p_j) = \hat{T}^n(p_j) + \Sigma_i \hat{W}_i(p_j)[\overline{\Theta}^n(\upsilon_i) - \Theta^n(\upsilon_i)] / \Sigma_i \hat{W}_i(p_j) \qquad (20)$$

where $\hat{T}(p_j)$ and $\hat{W}_i(p_j)$ are the mean values of $T(p)$ and $W_i(p)$ in layer p_j. There is no need for a one-to-one relationship between the number of channels and the number of layers.

In the GLA algorithm, layer mean temperatures between the mandatory levels [1000, 850, 700, 500, 400, 300, 200, 100, 70, 50, 30]

are used to determine the total temperature profile $T^{n+1}(p)$ at all pressure levels. This does not mean that we will determine ten pieces of information from the seven sounding frequencies used in the HIRS analysis. In fact, only six new pieces of information will be extracted from the HIRS channels (H2, H4, H13, H14, H15, M3, M4). To further minimize noise effects, the algorithm allows only six degrees of freedom in the solution and constrains all temperature profiles to be of the form

$$T_j^{n+1} = T'_j + \sum_{k=1}^{6} F_{jk} A_k^{n+1} \qquad (21)$$

where T'(p) is a global mean temperature profile, and $F_k(p)$ are empirical orthogonal functions, at 52 selected pressure levels extending from 1000 to 30 mb, given by the six eigenvectors with the largest eigenvalues of a set of global radiosondes profiles. The coefficients, A_k^{n+1}, uniquely define the solution in a given iteration. This approach is similar to the expansion used in Wark and Fleming (1966).

The six coefficients, A_k^{n+1}, can be determined at each iteration from the estimate of the ten layer mean temperature, T^{n+1} of the (n+1) iteration. Other ancillary information (if available) may be used to help determine the coefficients A_k^{n+1}.

In the GLA algorithm we find the six coefficients by a least squares solution of Eq. (21) for the ten specified layer-mean temperatures. The direct matrix solution is given by

$$A^{n+1} = (\hat{F}^* \hat{F})^{-1} \hat{F}^* \Delta^{n+1} \qquad (22)$$

where A is a vector of 6 coefficients and where $\hat{F}$ is a 10 by 6 matrix representing the mean value of F_{jk} in each of the ten mandatory layers, and Δ_j^{n+1} is equal to the difference between $\hat{T}_j^{n+1}$ and $\hat{T}'_j$ in the same ten mandatory layers according to the expression

$$\Delta_j^{n+1} = \hat{T}_j^{n+1} - \hat{T}'_j \qquad (23)$$

We use a constrained form [Rodgers, 1976]

$$A^{n+1} = [\hat{F}^* \hat{F} + \sigma H]^{-1} \hat{F}^* \Delta^{n+1} \qquad (24)$$

where H is a 6 by 6 matrix whose diagonal elements, H_{ii}, are the inverse of the fraction of total variance arising from eigenvector i, and

σ is a constant taken as $\sigma = 5 \times 10^{-4}$. This damps the coefficients of the higher order EOFs relative to those of the lower order EOFs.

The net result of Eqs. (20), (21), (23), and (24), is the iterative equation

$$T^{n+1} = T^n + [B - I][T^n - T'] + B\,W^n\,[\overline{\Theta}^n - \Theta^n] \qquad (25)$$

where T' is the 52 level global mean temperature profile, T^n is the nth guess temperature profile, $[\overline{\Theta}^n - \Theta^n]$ is the difference between reconstructed and computed clear column brightness temperature for the nth iteration, I is the identity matrix, W^n is the matrix of weighting functions in the nth iteration, as defined by Eq. (19) but normalized so that the sum of W over all channels equals 1 for any layer, and B is given by

$$B = F\,[\hat{F}^*\,\hat{F} + \sigma H]^{-1}\,\hat{F}^*\,\Lambda \qquad (26)$$

and Λ is the matrix which produces average values in the 10 mandatory layers as

$$\hat{T} = \Lambda T, \hat{F} = \Lambda F, \hat{W} = \Lambda W, \qquad (27)$$

The matrix BW is the basic interpolation matrix which estimates the necessary change in temperature profile to account for the difference between the observed and computed brightness temperture. BW is composed of two elements: (1) the profile dependent weighting functions which contain the atmospheric physics, and (2) the statistical matrix, B, which provides the constraints on the solution. The term $[B - I]\,[T^n - T']$ results from the expansion of the solution around the global mean temperature. This term would drop out of Eq. (25) if the expansion were made around the nth guess, T^n, rather than about the global mean. It should be noted here again that while Eq. (25) gives the temperature profile at 52 levels in the atmosphere, only 6 degrees of freedom are actually provided for the solution. Other structural information comes from the initial guess, in the form of first estimate of layer mean temperatures, and from the form of the EOFs.

While the form of Eq. (25) is similar to that used for statistical regression analysis, there are a number of significant differences. Foremost among these are that Eq. (25) contains the full physics of the radiative transfer equation in the term Θ^n, and allows for the incorporation of initial guess information into the solution in the term of T^n. In addition, it permits the physical treatment of the effects of

clouds on radiances in the term $\overline{\Theta}^n$, without requiring any field-of-view to necessarily to clear. Finally, the relaxation solution provides criteria to determine whether a solution can be found with satisfactory agreement with the observations in terms of $\overline{\Theta}^n - \Theta^n$.

6.1 Surface temperature

The sea-surface and ground-surface temperature can be expressed from Eq. (9) as

$$B(\upsilon_j,T_s)=\frac{1}{\varepsilon_s(\upsilon_j)}\left[\check{I}(\upsilon_j)/\tau(\upsilon_j,p_s)\right.$$

$$-\frac{\int_{p_s}^{0} B[\upsilon_j,T(p)]\frac{\partial\tau(\upsilon_j,p)}{\ln p}d\ln p}{\tau(\upsilon_j,p_s)} \qquad (28)$$

$$-\Omega\cos\theta\,[1-\varepsilon_s(\upsilon_j)]\,I_d(\upsilon_j,0)$$

$$\left.-H_h(\upsilon_j)\cos\phi_h\,\tau'(\upsilon_j,\phi_h,\theta)\,\rho_s(\upsilon_j,\phi_h,\theta)\right]$$

The surface temperature T_s appears in a nonlinear form in Eq. (28). The other unknowns are the surface emissivity ε and the solar bidirectional surface reflectivity ρ_s. We assume $T(p)$ and $\tau(p)$, which depends on the temperature and moisture profile, to be known in a given iteration. For the short wave windows at $4.0\mu m$ and $3.7\mu m$, we determine ρ_s in each iteration because uncertainties in its value can produce significant errors in T_s. The same uncertainties in ε, however, produce much smaller errors in T_s; therefore the emissivity is fixed in the analysis at typical values of 0.85 over land and 0.96 over ocean. For the $11\mu m$ channel, we assume a value for the surface emissivity equal to 0.95 for land and 0.98 for ocean, and neglect the contribution of reflected solar radiation. Solution of Eq. (28) for the determination of T_s is obtained by iteration. Details of the solution and acceptance criteria are given in Susskind et al. (1984) and Susskind et al. (1985).

6.2 Convergence criteria

Once convergence has been reached, in the sense that the residual,

$$R^n_{rms} = [\overline{\Theta}^n_i - \Theta^n_i]_{rms} \qquad (29)$$

for the temperature sounding frequencies used, are less than 0.95 of their value in the previous iteration, the retrieved solution is accepted

only if the residual is no greater than 1C. In addition, in order to check that the cloud filtering is accurate, the brightness temperature for MSU channel 2, calculated from the final profile must agree with the observation for this channel to at least 1C. This channel is sensitive to the average tropospheric temperature but is not used directly to retrieve $T(p)$. If either check fails, the profile is rejected as non-convergent.

7. COMPARISON WITH OPERATIONAL RETRIEVALS

The methods for analysis of HIRS2/MSU sounding data, described in the previous sections, differ in a number of important ways from those used operationally at NESDIS. The most prominent difference is the explicit use of physics in the GLA retrievals, in which expected radiances are computed as a function of geophysical and satellite viewing conditions and compared to observations. This step is not found either in the statistical retrievals, which until recently was performed operationally at NESDIS (Smith and Woolf, 1976), or in the new physical operational scheme (Fleming et al., 1986, 1988). The most important difference between the characteristics of the GLA retrievals and those produced operationally may in fact result from a step in the early stages of the operational processing system, the determination of the clear-column radiances used to produce the soundings.

The GLA retrievals perform all the radiative transfer calculations at the satellite zenith angle of observation (there is no zenith angle correction per-se) and the effects of clouds on the radiances are accounted for as part of the iterative procedure using Eqs. (9) - (13). NESDIS has taken a different approach toward accounting for the effects of clouds and varying satellite zenith angles on the observation. In a single step, preliminary to the retrieval itself, NOAA uses statistical relationships to convert potentially cloud contaminated radiances, observed at zenith angle θ, to clear-column radiances expected to be observed at nadir. These radiances are then used to produce the soundings. This procedure was used for the statistical operational retrievals, and is also used in the new physical operational retrieval scheme. The same clear-column radiances are also the ones written on the NESDIS level II tapes, and are commonly used to produce retrievals elsewhere.

This a-priori correction to nadir looking clear column radiances, which is not done in the GLA retrieval scheme, may in fact be the most

significant factor affecting differences between retrievals produced by the GLA approach and the NESDIS approach. Both the angle correction and the cloud correction to the observed radiances can be considerable. Moreover, the corrections depend in a complex way on not only the zenith angle and the cloud characteristics, but also the surface and atmospheric conditions.

The channel radiances represent integrals of atmospheric temperature structure. Given the correct integrals, any two approaches will provide basically the same solution, though fine structure will be different because of different constraints inherent in the assumptions used to invert the radiances. Errors in the clear column radiances produce errors in the integrals one is trying to solve. Therefore, this can result in large errors in the soundings. Thus, the biggest differences in retrievals produced by GLA and NOAA may be attributable more to the estimate of clear column radiances used in the inversion than to other details of the inversion scheme.

Before examining the accuracy of the GLA retrievals and NESDIS retrievals as a function of cloudiness, it is useful to look at the degree to which successful GLA retrievals can be performed as a function of cloudiness. On the average, about 59% of all retrievals for a 2 x 2 array of HIRS2 spots are accepted. Table 2 indicates a breakdown of the percent acceptance of GLA retrievals as a function of retrieved cloud fraction for the 2 x 2 array of spots. Cloud fields are always retrieved regardless of whether a successful temperature retrieval has been performed. Table 2 shows that the fraction of retrievals accepted is fairly constant with increasing cloudiness up to about 50% cloudiness, and even with 71%-80% cloudiness successful retrievals are produced about 45% of the time. Under some conditions, it is thought too cloudy to use equations (13) and (6) to produce clear column radiances for use in the retrieval process. Under these conditions, the area is considered too cloudy to generate a retrieval. The percent of time this occurs as a function of retrieved cloudiness is shown in the second row of the table. Retrievals are attempted under most cloud conditions. Attempted retrievals are rejected if the radiances computed from the solution do not match the cloud corrected radiances to a sufficient degree of accuracy. These solutions are referred to as non-convergent. The percentage of retrievals for each cloud fraction which are non-

Table 2 - Percentage acceptance of GLA Retrievals as a Function of Cloudiness

Cloud Fraction %	0	1-10	11-20	21-30	31-40	41-50	51-60	61-70	71-80	81-90	91-100
Per cent accepted	76.6	63.2	64.2	66.1	65.1	63.8	56.3	52.3	43.1	26.7	8.5
Too cloudy to try	0.0	0.0	0.0	0.0	0.2	0.9	4.1	8.1	14.7	28.8	40.0
non-convergent	21.2	31.7	27.7	25.0	24.8	27.0	28.7	29.3	31.2	29.4	29.0
Other reject	2.2	5.1	8.1	8.9	9.9	8.3	10.9	10.3	10.3	15.1	22.5

convergent is shown in the third row of the table. Surprisingly, this percentage is relatively independent of cloud fraction. Finally, retrievals are rejected for failure of other special tests which are described in Susskind et al., (1984). The fraction of time this occurs is shown in the last row of the table and is again relatively constant except for the lowest and highest cloud fractions.

We have examined the accuracy of the GLA retrievals and as a function of cloudiness and the results are shown in Table 3. Table 3 indicates the percentage of all retrievals which were accepted by the internal consistency check of the GLA system as a function of retrieved cloudiness, as well as the rms errors of layer mean temperatures compared to global collocated radiosondes within a ±3 hr time window and 110 km of the satellite location. Statistics are given for mostly clear cases, moderately cloudy cases, and cases of substantial cloudiness. rms errors are shown for 9 layers throughout the atmosphere and also for the two lowest layers for which results are most affected by clouds. rms errors for retrieved atmospheric layer mean temperatures between 10 mandatory level pressures covering the pressure range 50 mb - 1000 mb vary from 1.78°C for the clearest cases to 2.00°C for the cloudiest cases and do degrade somewhat with increasing cloudiness as might be expected because of the increased correction made to obtain clear column radiances in cloudiest cases. The accuracies in the two lowest levels of the atmosphere are somewhat poorer than the overall accuracy and appear to degrade faster with increasing cloudiness for moderate cloud amounts than the overall atmospheric rms errors, as may be expected. There is no apparent further degradation in accuracy in the lowest layers with further increase in cloudiness however.

Table 4 shows a breakdown of the accuracy of the operational NESDIS retrievals as a function of retrieval path for the same 10 day period. Paths A, B, and C can be thought of as representing increasing degrees of cloudiness. Retrievals labeled path A refer to cases in which the NESDIS cloud and angle correction algorithm identified an area in which no clouds were thought to be present, and only an angle correction were made to the observed radiances to obtain the radiances used for the retrieval. This occurred in roughly 48% of the retrievals reported. Path B retrievals refer to cases where both a cloud and an angle correction were made to the observed radiances to obtain the radiances used for

Table 3 - GLA Retrieval Characteristics as a Function of Cloudiness
NOAA 10 May 25-June 5, 1988

Percent cloudiness	0% - 10% essentially clear	10% - 40% moderately cloudy	40% - 100% cloudy
percent of retrievals	35%	30%	35%
rms errors (°C) 9 layers 1000 - 50 mb	1.78	1.93	2.00
rms errors (°C) 2 layers 1000 - 700 mb	2.08	2.45	2.44

Total number of retrievals ≈ 24000 profiles/day

Table 4. NESDIS Retrieval Characteristics as a Function of Path
NOAA 10 May 25-June 5, 1988

retrieval path	A Clear	B N*	C Microwave
percentage of retrievals	48%	25%	27%
rms errors (°C) 9 layers 1000 - 50 mb	1.80	1.85	2.51
rms errors 2 layers 1000 - 700 mb	2.12	2.61	4.38

Total number of retrievals ≈ 9600 profiles/day

the retrieval. This occurred roughly 25% of the time retrievals were reported. Path C refers to cases in which it was thought to be too cloudy to correct the tropospheric IR channels for cloud effects, and only angle corrected MSU and stratospheric sounding HIRS2 channel radiances

were used in the retrieval. This occurred about 27% of the time. Such "microwave only" retrievals are not produced by the GLA system because of the poor vertical resolution of the MSU instrument in the troposphere. If we examine results as a function of cloudiness, it is apparent that the accuracy of NESDIS path A retrievals is comparable to that the GLA retrievals under essentially clear conditions, and that of the path B retrievals are of comparable accuracy to the GLA retrievals under moderate cloud conditions. On the other hand, path C retrievals, are of considerably poorer accuracy than GLA retrievals under cloudy conditions, especially in the lower troposphere. We attribute this difference to the ability of the GLA retrieval to utilize HIRS2 observations effectively even under very cloudy conditions. The accuracies shown in table 4 are for the NESDIS statistical retrievals performed operationally at that time. NESDIS physical retrievals were also performed experimentally at that time and their accuracies are not appreciably different from the values shown in table 4. The physical retrievals used the same cloud and angle corrected radiances as the statistical ones, including the path C radiances.

It is informative to examine the distribution of retrievals produced by both GLA and NESDIS as a function of retrieval type and retrieved cloud fraction. This distribution is shown for a six hour period in Figures 3 and 4 for NESDIS and GLA retrievals respectively. Each area represents a 4° latitude by 5° longitude grid box. If any successful retrievals were reported in a box, an appropriate letter is shown. For NESDIS, A is shown if any retrievals in the box were type A, B is shown if there were no type A but at least one type B retrieval, and C is shown if only C type retrievals were performed. Areas in which no retrievals were reported are left blank, but appear as a dot if the area was over land. A total of 2448 retrievals was reported for the 6 hour period, with a breakdown of A, B, and C types as indicated on the figure. Figure 4 shows analogous results for GLA retrievals. Only areas containing at least one successful retrieval in a grid box are marked with a letter. The letters A, B, and C are used to represent retrievals under cloud conditions 0 - 10%, 11 - 40%, and 41 - 100% respectively, so as to be analogous to increasing cloudiness as implied by the NESDIS retrieval type. As in Figure 3, if any retrievals in a grid box were A, the letter A is shown. Otherwise, B takes precedence, and C is used if only retrievals in greater than 40% cloudiness were obtained. A total of 5932 successful retrievals were performed in this time period, with a

breakdown as a function of retrieved cloud conditions indicated in the figure. Also shown is the total number of retrievals attempted.

A number of aspects of the two retrieval schemes are apparent from Figures 3 and 4. Figure 3 shows some large areas containing only path C (microwave only) retrievals, which have been shown to have very poor error characteristics. Note, for example, the area in the Atlantic Ocean at 35W - 45W, 38N - 54N and the area near Japan around 140E, 38N. Even though the GLA system produces successful retrievals less often under extremely cloudy conditions, there are no appreciable data gaps in these regions in the GLA retrievals and most of the retrieved cloudiness is actually in the range 10% - 40% in these areas. In fact, even though roughly 40% of the sounding areas do not result in successful retrievals, very few data gaps are seen in the Figure 4. That is because a large majority of the rejected retrievals occur at high latitudes. We are currently examining the cause of this.

Systematic gaps are observed near the equator in Figure 4, which are even larger in Figure 3. The gaps in Figure 4 are a result of the fact that the scan patterns of successive orbits do not overlap until about 30° poleward of the equator. The maximum side scan angle of HIRS2 is 49.5°, corresponding to a satellite zenith angle of 60°. A maximum side scan angle of 55°, such as found in the imaging AVHRR instrument on the NOAA satellites, would be sufficient to provide full coverage at the equator. This larger viewing angle was not incorporated into the sounding instruments because of concern by NOAA about the quality of soundings at large zenith angles.

It is apparent from the size of the gaps near the equator in Figure 3 that NOAA does not report soundings in areas observed at larger zenith angles by the HIRS2/MSU instruments. It is apparent also that C type retrievals often occur at the end of a scan line. These two findings are indicative of problems arising from large a-priori zenith angle corrections, especially in the presence of clouds.

We were not able to examine the dependence of the accuracy of the NESDIS retrievals as a function of satellite zenith angle because this is not a reported quantity. We did examine the dependence of the GLA retrieval accuracy and percent acceptance on the satellite zenith angle, and the results are shown in table 5. The results show some decrease

DISTRIBUTION OF NESDIS RETRIEVALS

NOAA 10 MAY 15, 1988 9Z - 15Z

TYPE	NUMBER
A	1172
B	626
C	650
TOTAL	2448

Figure 3 Distribution of reported operational retrievals for a six hour period. Results are shown on a 4° x 5° grid. A means at least one A type retrieval in a grid; B means no A type but at least one B type; C means C type only. Areas with no data are left blank.

DISTRIBUTION OF GLA RETRIEVALS

NOAA 10 MAY 15, 1988 9Z - 15Z

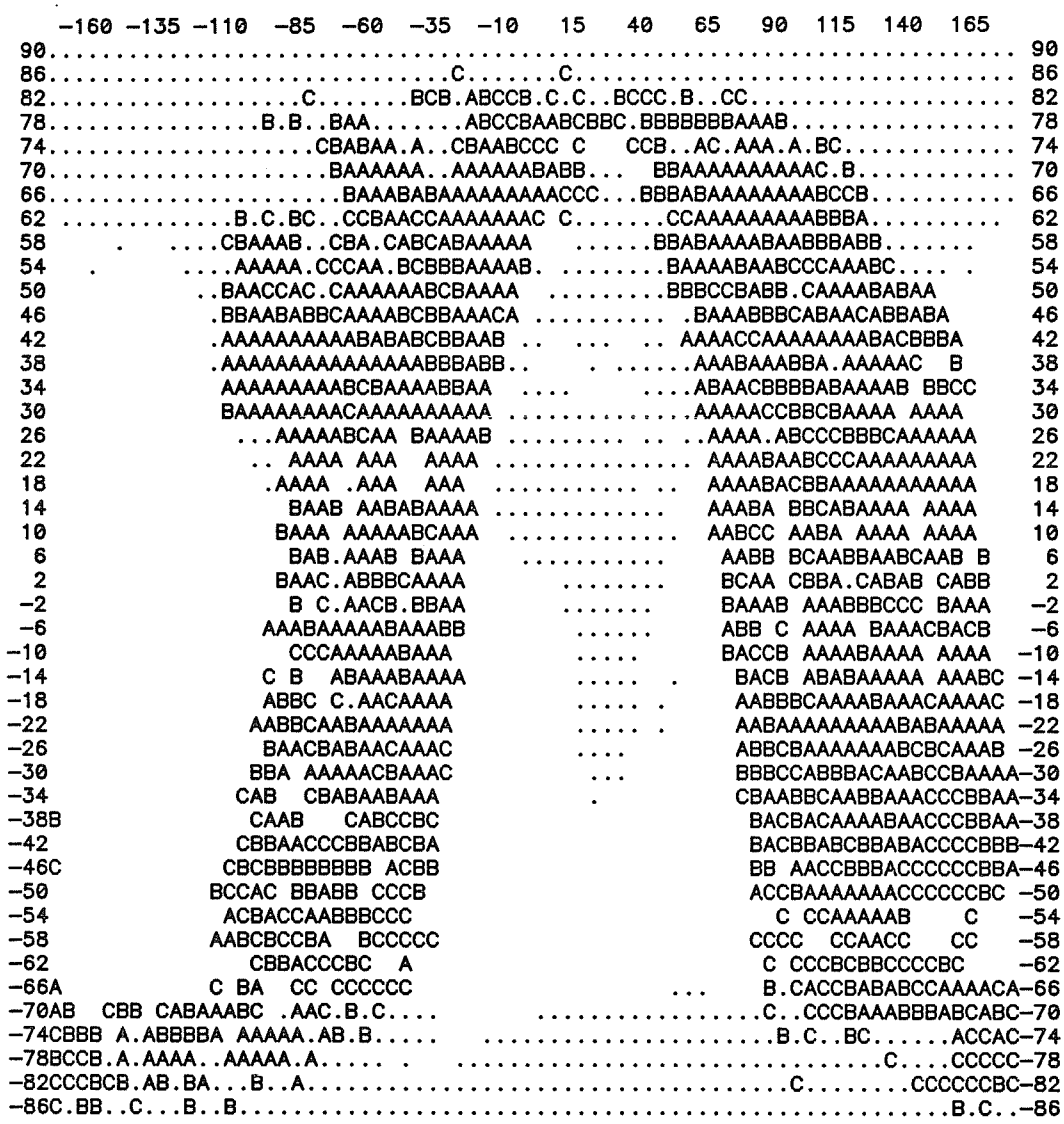

TYPE	NUMBER
A	2071
B	1768
C	2093
TOTAL ACCEPTED	5932
TOTAL	10389

Figure 4 Distribution of GLA retrievals for a six hour period. Results shown on a 4° x 5° grid. A means at least one retrieval with $\alpha \leq 0.1$; B means no A but at least one retrieval with $0.1 < \alpha \leq 0.4$; C means $\alpha > 0.4$ for all retrievals. Areas with no data are left blank.

Table 5 - Accuracy of GLA Retrievals vs Satellite Zenith Angle
NOAA 10, May 24 - June 4, 1988

Zenith angle	0°-10°	10°-20°	20°-30°	30°-40°	40°-50°	>50°	All GLA	All NESDIS
percent accepted	62.5	62.0	61.8	60.7	56.9	52.2	58.5	
RMS error (°C) 9 layers 1000mb - 50mb	1.85	1.79	1.86	1.93	2.03	2.01	1.90	1.94
RMS error (°C) 2 layers 1000mb - 700mb	2.22	2.08	2.19	2.38	2.38	2.60	2.28	2.82

in yield and accuracy at angles greater than 30°, but the accuracy of retrievals with zenith angle greater than 50° is still better at lower levels than that of the entire ensemble of NESDIS retrievals, which is also shown in table 5. We attribute the small decrease in accuracy at large zenith angles to the very large size of the MSU footprint at the end of the scan pattern. This would hinder the treatment of cloud effects at large angles. This problem will be alleviated considerably when MSU is replaced operationally in the future with AMSU, which has twice the spatial resolution of MSU. These results suggest that not only will accurate retrievals be produced from HIRS/AMSU at side scan angles of 49°, but that potentially accurate retrievals could be produced at 55°, which would provide full coverage at the equator. Increasing the scan angle to 55° would represent a minor modification to the design of the AMSU instrument which would further improve sounding capability when AMSU is launched in the early to mid 1990's if such a change were incorporated into its design.

8.0 REFERENCES

Chahine, M. T., 1968: Determination of the Temperature Profile in an Atmosphere from its Outgoing Radiance, J. Opt. Soc. Amer., 58, 1634-1637.

Chahine, M. T., 1970: Inverse Problems in Radiative Transfer, J. Atmos. Sci., 27, 960-967.

Chahine, M. T., 1974: Remote Sounding Cloudy Atmospheres. I. The Single Cloud Layer, J. Atmos. Sci., 31, 233-243.

Chahine, M. T., 1977: Remote Sounding in Cloudy Atmospheres. II/ Multiple Cloud Formations. J. Atmos. Sci., 34, 744-757.

Chahine, M. T., 1982: Remote Sensing of Cloud Parameters, J. Atmos. Sci., 39, 159-170.

Fleming, H. E., M. D. Goldberg, and D. S. Crosby, 1986: Minimum Variance Simultaneous Retrieval of Temperature and Water Vapor from Satellite Radiance Measurements. Preprints 2nd Conference on Satellite Meteorology/Remote Sensing and Applications, 13-16 May, Williamsburg, VA. Am. Met. Soc. Boston pp. 20-23.

Fleming, H. E., M. D. Goldberg, and D. S. Crosby, 1988: Operational Implementation of the Minimum Variance Simultaneous Retrieval Method. Preprints 3rd Conference on Satellite Meteorology and Oceanography, 31 Jan. - 5 Feb., Anaheim Calif., Am. Met. Soc., Boston, pp. 16-19.

Kalnay, E. R., R. Bolgovind, W. Chao, D. Edelmann, J. Pfaendtner, L. Takacs, and K. Takano, 1983: Documentation of the GLAS Fourth Order General Circulation Model, NASA Technical Memorandum 86064, [NTIS N8424028].

Phillips, N., J. Susskind, L. McMillin, 1988: Results of a Joint NOAA/NASA Sounder Simulation Study, J. Atmos. and Ocean Tech., 5, No. 1, 44-56.

Reuter, D., J. Susskind, and A. Pursch, 1988: First Guess of Physically Based Temperature-Humidity Retrievals from HIRS/MSU DATA, J. Atmos. Ocean Tech., 5, 70-83.

Rodgers, C. D., 1976: Retrieval of Atmospheric Temperature and Composition from Remote Measurements of Thermal Radiation, Rev. Geophys. Space Phys., 14, 609-624.

Smith, W. L., and H. M. Woolf, 1976: The use of Eigenvectors of Statistical Covariance Matrices for Interpreting Satellite Sounding Radiometer Measurements. J. Atmos. Sci., 33, 1127-1140.

Susskind, J., J. Rosenfield, and D. Reuter, 1983: An Accurate Radiative Transfer Model for use in the Direct Physical Inversion of HIRS2 and MSU Temperature Sounding Data. J. Geophys. Res., 88, 8550-8568.

Susskind, J., J. Rosenfield, D. Reuter, and M. Chahine, 1984: Remote Sensing of Weather and Climate Parameters from HIRS2/MSU on TIROS-N, J. Geophys. Res., 89, No. D3, 4677-4697.

Susskind, J., and D. Reuter, 1985: Retrieval of Sea Surface Temperatures from HIRS/MSU Data, J. Geophys. Res., 90C, 11602-11608.

Susskind, J., D. Reuter, and M. T. Chahine, 1987: Cloud Fields Retrieved from HIRS/MSU Data, J. Geophys. Res., 92D, 4035-4050.

Wark, D. Q., and H. E. Fleming, 1966: Indirect Measurements of Atmospheric Temperature Profiles from Satellites, 1, Introduction, Mon. Weather Rev., 95, 351-362.